water

MDPI

Article

A Simplified Analytical Method to Predict Shallow Landslides Induced by Rainfall in Unsaturated Soils

Antonello Troncone *, Luigi Pugliese and Enrico Conte

Department of Civil Engineering, University of Calabria, 87036 Rende, Cosenza, Italy; luigi.pugliese@unical.it (L.P.); enrico.conte@unical.it (E.C.)
* Correspondence: antonello.troncone@unical.it

Abstract: In order to assess slope stability owing to rainfall, the availability of an effective and simple-to-use methodology, relating directly rain to eventual landslide triggering, is undoubtedly useful. To this purpose, a simplified method aimed to the prediction of rainfall-induced shallow landslides in unsaturated soils is proposed in the present study. This method takes advantage of some closed-form solutions to evaluate the change in pore pressure due to infiltration of a rainfall characterized by a given intensity and duration, and the simple scheme of infinite slope to calculate a threshold for the change in pore pressure when the slope is under limit conditions. Particularly, using the present approach, a critical curve can be defined to establish the rainfall events that can trigger a failure process at a given depth, where suction before rainfall is known. The proposed method appears promising from an engineering viewpoint, since it is simple to use and requires few parameters as input data. In addition, these parameters can be determined from conventional geotechnical tests. The validity of the proposed approach is corroborated by some comparisons with the results of well-documented case studies.

Keywords: rainfall-induced shallow landslides; unsaturated soil; simplified method; intensity–duration critical curve

Citation: Troncone, A.; Pugliese, L.; Conte, E. A Simplified Analytical Method to Predict Shallow Landslides Induced by Rainfall in Unsaturated Soils. *Water* **2022**, *14*, 3180. https://doi.org/10.3390/w14193180

Academic Editor: Marco Franchini

Received: 29 August 2022
Accepted: 6 October 2022
Published: 9 October 2022

1. Introduction

Rainfall-induced shallow landslides generally occur during short and intense rainstorms or after long rainy periods, depending on the infiltration capacity of the slope and soil properties (mainly hydraulic conductivity and saturation degree), in relation to rainfall intensity and duration. The thickness of the unstable soil typically ranges from some decimeters to few meters (generally 1–2 m). Movement usually experienced by these landslides is a translational slide [1] with direction mainly parallel to the ground surface. However, under certain conditions, these landslides evolve into debris flows [2–7]. Therefore, despite the relatively small volume of the displaced material, such landslides could be really dangerous due also to the lack of warning signs that make problematic their prediction. In view of these features, rainfall-induced landslides have caught the interest of the scientific community in recent decades. As a result, many studies were published in the literature on this topic [8–20].

Landslide triggering is strictly related to the condition of partial saturation of the soil in the shallow portion of the slope, a condition that favors slope stability because suction gives a sort of apparent cohesion to the soil, resulting in an increase of its shear strength. However, rain infiltrating into the slope causes a progressive reduction of suction (and consequently of soil strength) that could lead to slope instability [21]. Therefore, the most critical situation for slope stability occurs when small values of suction exist in the soil before rainfall commences. This mainly occurs owing to prolonged rainfall periods that cause an increase in soil water content up to levels close to saturation. This may also occur during the formation of a capillary barrier in an unsaturated soil layer lying on a soil with

higher permeability [22]. In these circumstances, water is retained in the upper layer and consequently, its saturation degree increases causing a reduction in the soil shear strength. Therefore, it is undeniable that the effects of rain infiltration on the pore water pressure regime cannot be ignored for the analysis of rainfall-induced landslides [23–26].

Although numerical solutions based for example on the finite element method or the finite difference method, can provide a comprehensive understanding of the complex infiltration and deformation processes occurring in the slope [27–36], the availability of simplified (but reliable) methods is undoubtedly useful to readily assess slope stability, especially for shallow landslides that generally involve relatively small volumes of displaced material in comparison with other types of landslides.

From a general point of view, the critical stability condition of a slope due to rainfall can be achieved as a result of a decrease in suction or a subsequent increase in the positive pore pressure, depending on the hydrological characteristics of the soil and the rainfall intensity. This means that, from a phenomenological point of view, the failure surface can form within either the unsaturated or saturated portion of the slope. However, only the case in which the failure surface develops in the unsaturated portion of the slope is considered in the proposed method. In this context, a user-friendly method is proposed in the present study for predicting the occurrence of rainfall-induced shallow landslides in unsaturated soils. Specifically, the method is based on some closed-form solutions to evaluate the changes in pore water pressure due to rain infiltration, and the infinite slope model to calculate a threshold value for pore water pressure corresponding to a limit condition of the slope. A critical rainfall intensity-duration relationship is also obtained, which can be readily used to predict whether (or not) a landslide occurs owing to expected rainfall scenarios. Another advantage of the present approach is that few parameters, derived from conventional geotechnical tests, are required as input data. However, the proposed method is affected by some approximate assumptions that have to be kept in mind when it is applied to real cases, as specified in the subsequent sections. In addition, some effects are ignored [37,38]. Application to some real cases study is performed to assess the validity of the proposed method.

2. Method of Analysis

The differential equation governing rain infiltration into an infinite slope consisting of unsaturated soils (Figure 1) can be written as follows, under the assumption that air is at atmospheric pressure and soil properties are constant [39]:

$$\frac{\partial u_w}{\partial t} = c_w \frac{\partial^2 u_w}{\partial z^2} \tag{1}$$

where u_w is the change in pore water pressure (otherwise suction) caused by rain infiltration at time t and depth z (measured normally to the ground surface), with respect to the suction existing at the same depth before rainfall commences. This latter is herein indicated with u_{wo}. It takes a negative value for unsaturated soils and should be determined from in situ measurements, using tensiometers. By contrast, u_w assumes positive values. The parameter c_w takes the form:

$$c_w = \frac{k}{\gamma_w m_w} \tag{2}$$

in which γ_w is the unit weight of water, k is the soil hydraulic conductivity, and m_w is the coefficient of water volume change with respect to a change in suction, which is provided by the slope of the retention curve at a given suction [21]. An evaluation of m_w can be performed by measurements of dilational and shear wave velocities (V_P and V_S), as proposed by [40,41].

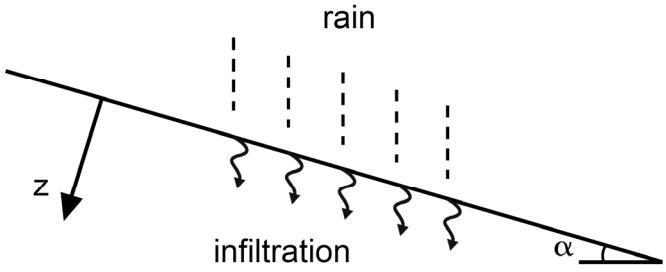

Figure 1. Scheme used for the analysis of the rain infiltration process in an infinite slope.

Actually, m_w and k depend on the position and suction. However, in view of developing a method of practical interest, in the present study it is assumed, as an approximation, that these parameters remain unchanged during the infiltration process. In this connection, m_w is evaluated as the slope of the retention curve at the initial suction u_{wo}, and k is cautiously assumed equal to the saturated hydraulic conductivity of soil [42]. This choice, in fact, leads to the highest rain infiltration and the highest u_w.

To solve Equation (1), the following initial and boundary conditions are considered:

$$u_w = 0 \quad \text{for} \quad t = 0 \quad \text{and} \quad \forall z \tag{3}$$

it expresses the condition that at t = 0 the change in pore water pressure is nil everywhere (initial condition);

$$\frac{\partial u_w}{\partial z} = -\frac{\gamma_w}{k} I \quad \text{for} \quad z = 0 \quad \text{and} \quad t > 0 \tag{4}$$

where I denotes the rain infiltration at the slope surface (boundary condition at z = 0);

$$u_w(\infty, t) = 0 \quad \text{for} \quad t > 0 \tag{5}$$

this equation expresses the boundary condition that the change in suction due to rain infiltration is nil at high depths. Considering a rainfall event characterized by a constant intensity R and duration d, I can be expressed as:

$$I = R \quad \text{if} \quad R < p \quad \text{and} \quad t \leq d \tag{6a}$$

$$I = p \quad \text{if} \quad R \geq p \quad \text{and} \quad t \leq d \tag{6b}$$

$$I = 0 \quad \text{if} \quad t > d \tag{6c}$$

where p is the potential infiltration rate, which is the maximum volume of water (per unit area) that can infiltrate into the soil in a time unit. Generally, p is influenced by many factors that make very difficult its evaluation, such as previous rainfall, presence of vegetation, evapotranspiration, tension cracks, preferential drainage paths, etc. [43–45]. To this end, field tests should be carried out. Nevertheless, for a preliminary evaluation of this parameter, this approximate equation could be used [46]:

$$p = k \cos \alpha \tag{7}$$

where α is the slope angle of the ground surface.

On the basis of the initial and boundary conditions (Equations (3)–(5)), a closed-form solution of Equation (1) can be derived [47,48]:

$$u_w(z, t) = \frac{2\gamma_w I}{k} \left[\sqrt{\frac{c_w t}{\pi}} e^{-\frac{z^2}{4c_w t}} - \frac{z}{2} erfc\left(\frac{z}{2\sqrt{c_w t}} \right) \right] \quad \text{for} \quad t \leq d \tag{8a}$$

$$u_w(z,t) = \frac{2\gamma_w I}{k}\left[\sqrt{\frac{c_w t}{\pi}}e^{-\frac{z^2}{4c_w t}} - \frac{z}{2}erfc\left(\frac{z}{2\sqrt{c_w t}}\right)\right] + \\ -\frac{2\gamma_w I}{k}\left[\sqrt{\frac{c_w (t-d)}{\pi}}e^{-\frac{z^2}{4c_w (t-d)}} - \frac{z}{2}erfc\left(\frac{z}{2\sqrt{c_w (t-d)}}\right)\right] \quad \text{for} \quad t > d \tag{8b}$$

where $erfc$ is the complementary error function. Summarizing, Equations (8a) and (8b) provide the change in pore water pressure occurring at any depth and time owing to a rain event characterized by an infiltration rate I and duration d. Equation (8a) is an increasing monotonic function, therefore the maximum value of u_w is attained at $t_p = d$. Referring to Equation (8b), the time corresponding to the maximum value of u_w is determined by imposing that:

$$\frac{\partial u_w}{\partial t} = 0 \tag{9}$$

To this aim, it is convenient to write Equation (8b) in the following form [48]:

$$\frac{\psi}{z} = \frac{I}{k}[R(t^*) - R(t^* - d^*)] \tag{10}$$

in which $\psi(z,t) = u_w(z,t)/\gamma_w$ is the pressure head, and:

$$t^* = \frac{4c_w t}{z^2} \tag{11}$$

$$d^* = \frac{4c_w d}{z^2} \tag{12}$$

$$R(t^*) = \sqrt{\frac{t^*}{\pi}}e^{-\frac{1}{t^*}} - erfc\left(\frac{1}{\sqrt{t^*}}\right) \tag{13}$$

As a result, Equation (9) takes the form:

$$e^{\left[\frac{z^2}{4c_w}\left(\frac{d}{t_p(t_p-d)}\right)\right]} = \frac{\sqrt{t_p}}{\sqrt{t_p - d}} \tag{14}$$

which can be solved to provide the time t_p when the maximum value of u_w is attained after the end of rainfall. It is worthwhile noting that t_p depends on the rain duration, but it does not depend on the rainfall intensity. Figure 2 relates t_p to d, for different values of $a = z^2/4c_w$.

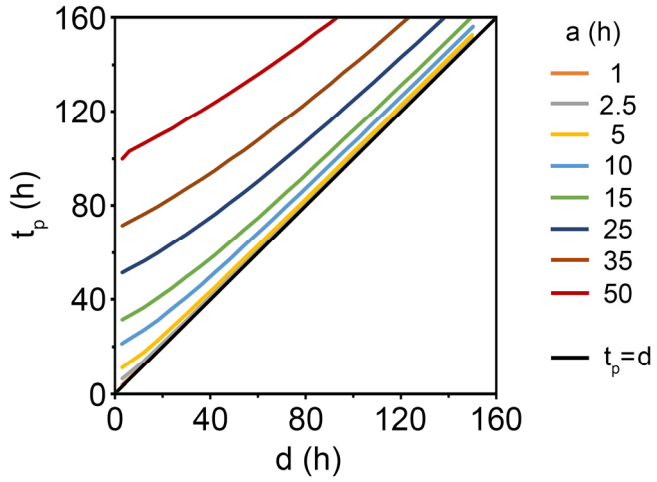

Figure 2. Relationship between t_p and d, for different values of a.

As can be seen, t_p approaches d for small values of a, i.e., at shallow depths and/or for high values of c_w (or highly permeable soils). By contrast, t_p could be significantly greater

that d at high depths and for poorly permeable soils. Consequently, depending on depth and hydraulic conductivity, the evolution of u_w with time assumes a different shape, as shown in Figure 3. In this figure, the blue curve corresponds to a case with $t_p = d$, and the red curve is representative of a case when $t_p > d$. A slope failure could occur before the end of the rainfall in the first case, whereas failure likely occurs after the rainfall event in the second case.

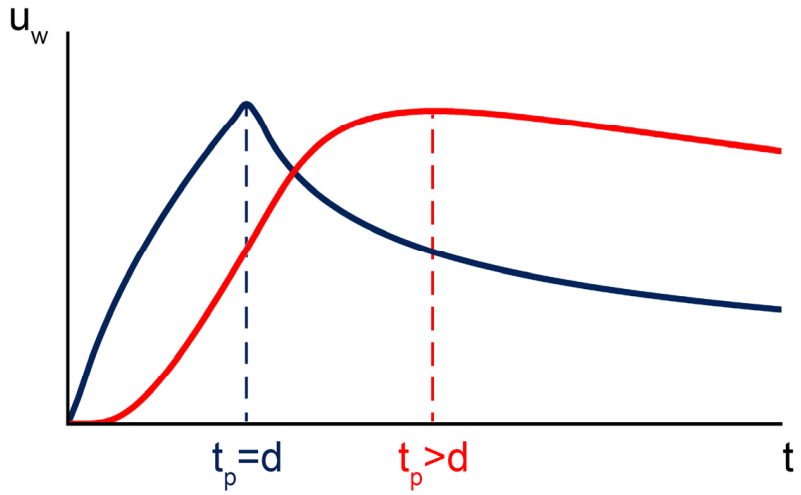

Figure 3. Evolution of u_w with time when $t_p = d$ (blue curve) and when $t_p > d$ (red curve).

Indeed, a landslide is triggered if the maximum value of u_w exceeds a threshold value, u_c. This latter is determined by imposing that the safety factor of the slope is unit at a given depth z [30]:

$$FS = \frac{c' + \gamma z \cos\alpha \tan\phi' - \chi(u_{wo} + u_w)\tan\phi'}{\gamma z \sin\alpha} = 1 \quad (15)$$

In Equation (15), c' and ϕ' are the effective cohesion and the angle of shearing resistance of the soil, respectively, χ is a parameter ranging between 0 and 1 depending on the water content [46], which in turn depends on the matric suction [49], and γ is the unit weight of the soil. For simplicity, in the present study it is assumed that $\chi = 1$ and γ is constant, considering that this latter is generally slightly affected by infiltration. The resulting expression of u_c is:

$$u_c = \frac{1}{\tan\phi'}\left[c_t - \gamma z\left(\sin\alpha - \cos\alpha \tan\phi'\right)\right] \quad (16)$$

in which:

$$c_t = c' - u_{wo}\tan\phi' \quad (17)$$

At this point, by imposing:

$$u_w\left(z_s, t_p\right) = u_c \quad (18)$$

it is possible to determine, for a certain duration d, a critical value of the rainfall infiltration rate, I_{crit}, which is capable to trigger a landslide at a certain depth z_s where the initial suction u_{wo} is known. From a general point of view, the value of u_{wo} appearing in Equation 15 can be either negative or positive and, consequently, the critical condition can be reached as a consequence of the reduction of suction or increase in the positive pore water pressure. However, the proposed method is suitable for the prediction of shallow landslides triggering due to rainfall only when the failure surface develops in the unsaturated portion of the slope. In this case, the soil is in the unsaturated condition before rainfall and, consequently, u_{wo} takes a negative value. For a more generic situation, in which u_{wo} can be either negative or positive, a different method should be employed [19,20].

After substituting Equations (8b) and (16) into Equation (18), the following expression of I_{crit} is obtained:

$$I_{crit} = \frac{u_c k}{2\gamma_w} \cdot \frac{1}{R(\bar{t}) - R(\bar{t} - \bar{d})} \tag{19}$$

where

$$\bar{t} = \frac{4c_w t_p}{z_s^2} \tag{20}$$

and

$$\bar{d} = \frac{4c_w d}{z_s^2} \tag{21}$$

It is worth noting that $R\left(\bar{t} - \bar{d}\right)$ approaches zero as t_p approaches d, leading to the same result obtained using Equation (8a) instead of Equation (8b) when $t_p = d$. In other words, Equation (19) is a general equation that can be used both for $t_p = d$ and $t_p > d$.

Calculating I_{crit} for different values of d, a critical curve is obtained (Figure 4) which allows the stability condition of a slope to be readily assessed on the basis of intensity R and duration d of an expected rainfall. Nevertheless, since a portion of rainfall can generally infiltrate into the slope taking into account the potential infiltration rate (Equations (6a) and (6b)), it is convenient to calculate a critical duration, d_c, using Equation (19) in which the condition $I_{crit} = p$ is imposed. As a result, if an expected rainfall is characterized by a duration $d < d_c$, the slope is stable independently on the expected rainfall intensity R, making the concept of critical duration very useful from a predicting point of view. Contrariwise, a landslide occurs if $d \geq d_c$ (i.e., if the rainfall is sufficiently prolonged in time), provided that $I \geq I_{crit}$. In other words, a landslide can be triggered only if the point representative of an expected rainfall with intensity R and duration d, falls into the area highlighted in red in Figure 4. As shown in the flow chart of Figure 5, the solution procedure is very simple-to-use and is hence suitable for routine applications.

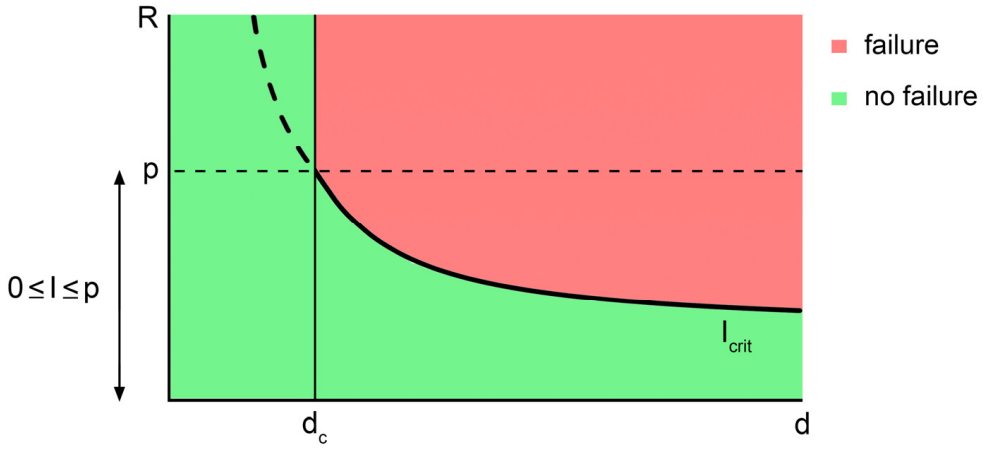

Figure 4. Example of critical curve.

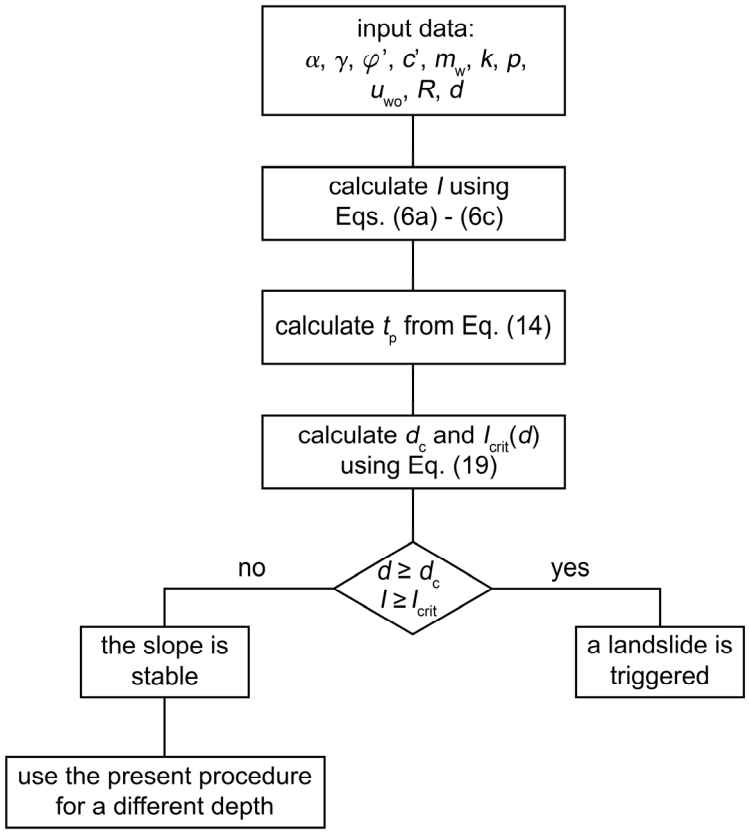

Figure 5. Flow chart illustrating the use of the proposed method. The critical duration, d_c, is calculated using Equation (19) in which $I_{crit} = p$ is imposed.

3. Application of the Method

In this section, the proposed method is applied to analyze two case studies documented in the literature.

The first case study is drawn from a paper by [50] and concerns a rainfall-induced shallow landslide occurred in a site near the city of Bologna (Northern Italy). The slope can be schematized as an infinite slope with an average inclination $\alpha = 14°$. It was affected in the past by landslide movements that involved an inorganic clay with high plasticity [51]. Two failure surfaces were localized at the depths (measured in the vertical direction) of 0.80 m ($z = 0.78$ m) and 1.40 m ($z = 1.36$ m), respectively [50]. Direct shear tests performed on reconstructed samples provided a residual friction angle $\varphi' = 12°$ and a nil intercept cohesion. Additional strength contributions due to the presence of roots can be neglected at the depths where the slip surfaces were found [51]. The measured hydraulic conductivity was $k = 4.6 \times 10^{-7}$ m/s. Since no infiltration tests was carried out, the potential infiltration rate is approximately evaluated using Equation (7) that provides $p = 38.4$ mm/day. Experimental data concerning the volumetric water content ϑ and suction s are documented by [50]. To determine a retention curve for the soil involved in the landslide, these data are fitted using the following relationship, which was originally proposed by [52] and subsequently modified by [53]:

$$\frac{\vartheta - \vartheta_R}{\vartheta_S - \vartheta_R} = \left[\frac{1}{1 + (\beta s)^n}\right]^{1-\frac{1}{n}} \tag{22}$$

where ϑ_S is the volumetric water content at saturation, ϑ_R is the residual volumetric water content, and β and n are model parameters. Table 1 reports the values of these parameters that provided the best agreement between experimental data and Equation (22),

as documented in Figure 6. Once the retention curve is obtained, the coefficient of water volume change m_w is evaluated as the slope of this curve at the initial suction u_{wo}.

Table 1. Van Genuchten model's parameters (data drawn from [50]).

ϑ_R	ϑ_S	β (kPa^{-1})	n
0.07	0.54	0.095	1.3

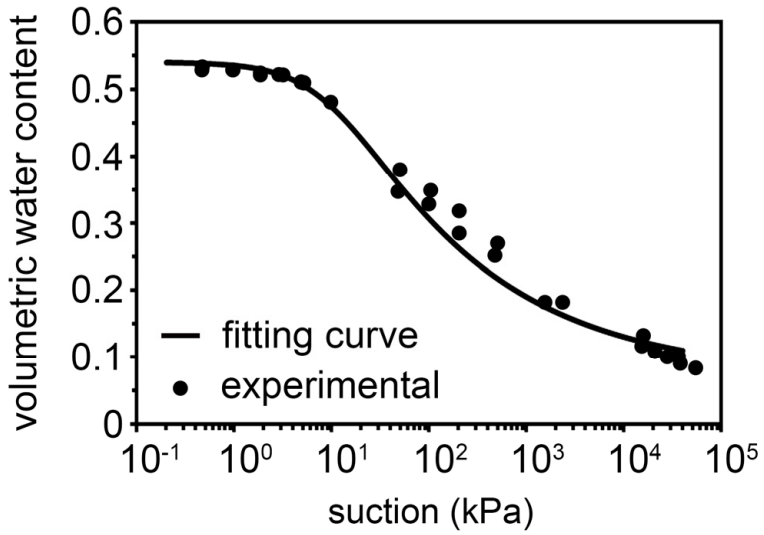

Figure 6. Comparison between the theoretical retention curve (Equation (22)) and some experimental data obtained from laboratory tests (modified from [50]).

Daily rainfall recorded from October 2004 to August 2006 are available (Figure 7). The present method is used to analyze the slope response to three rainfall events, which are indicated by red arrows in Figure 7. It is worth noting that the rainfall event characterized by the highest value of intensity (about 140 mm/day) in Figure 7 was not considered in the present study because it did not cause any failure mechanism due to the very high value of suction measured before this event (about 1000 kPa). Rain intensity, initial suction (measured just before these events) and the associated values of m_w are included in Table 2. Duration of each event is 24 h.

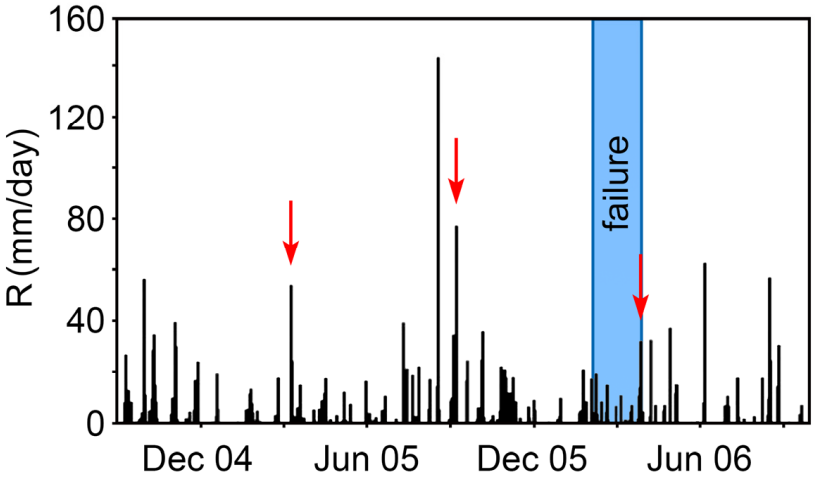

Figure 7. Available rainfall recordings (modified from [50]).

Table 2. Rainfall intensity and initial suction for the events considered in the analyses (data drawn from [50]), along with the corresponding values of m_w.

Rainfall	R (mm/day)	u_{wo} (kPa)	m_w (kPa^{-1})
10 April 2005	54	−33	0.0036
5 October 2005	77.5	−40	0.0019
1 May 2006	32.5	−4.9	0.0072

The values of suction in Table 2 are those measured at the depth of 0.80 m, where the upper slip surface was detected. Since no measurement is available at the depth of 1.40 m, where the lower slip surface was detected, the values of suction measured at 0.80 m are also assigned to the depth of 1.40 m. This assumption is justified by the fact that the available measurements provide an essentially constant profile of suction with depth [50].

As documented by [50], some instability phenomena were observed in the period March–May of 2006 (Figure 7). Therefore, only the third rainfall event among those considered in the present study caused a slope failure at the above-mentioned depths (0.80 m and 1.40 m).

Figures 8–10 present the critical curves calculated at the depth of 0.80 m using the procedure described in the previous section, for each value of u_{wo} measured at this depth (Table 2). As can be seen, no slope failure occurs owing to the first rainfall events considered (Figures 8 and 9). In this case, in fact, the rainfall duration d is always less than the critical threshold d_c, the values of which are indicated in Table 3. In addition, since the rainfall intensity is greater than the potential infiltration rate ($R > p$), a portion of the rainfall infiltrates into the slope (Equations (6a) and (6b)).

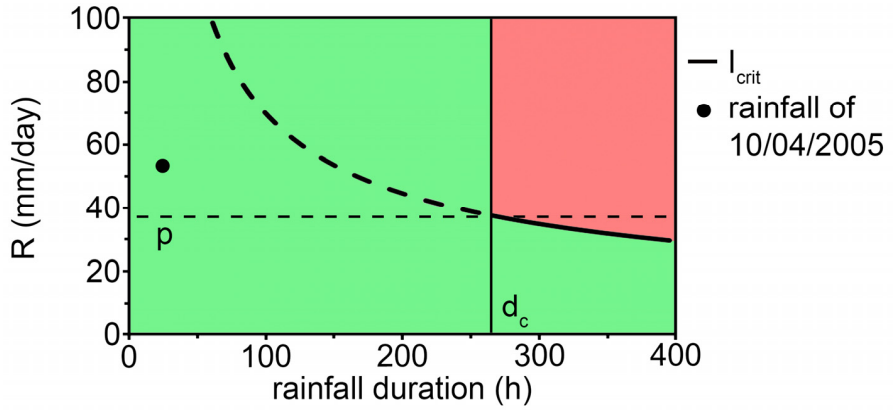

Figure 8. Comparison between the rainfall event recorded on 10 April 2005 and the critical curve calculated at the depth of 0.80 m.

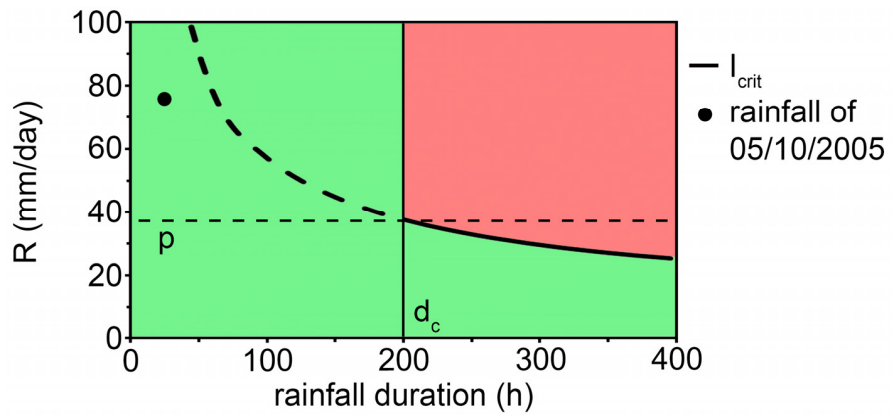

Figure 9. Comparison between the rainfall event recorded on 5 October 2005 and the critical curve calculated at the depth of 0.80 m.

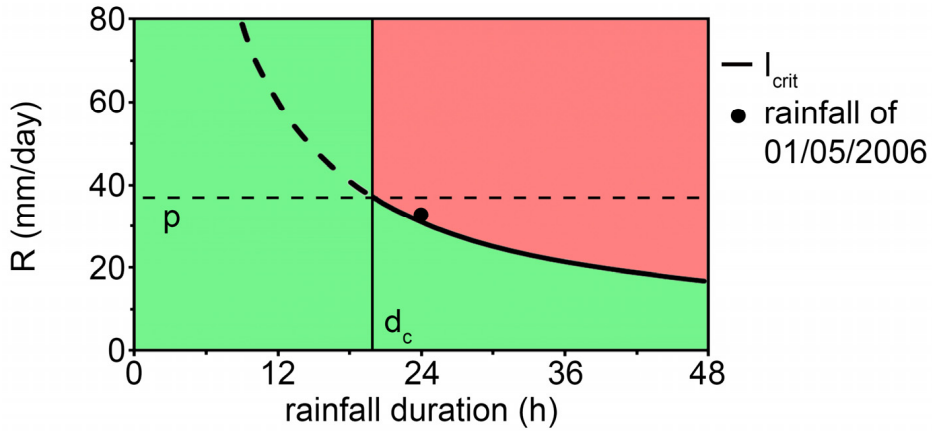

Figure 10. Comparison between the rainfall event recorded on 1 May 2006 and the critical curve calculated at the depth of 0.80 m.

Table 3. Values of the critical duration d_c (in hours) calculated considering the initial suction existing before the considered rainfall events.

	10 April 2005	5 October 2005	1 May 2006
z_s = 0.80 m	264	200	20
z_s = 1.40 m	305	227	10

By contrast, rainfall totally infiltrates into the slope when the third event is considered ($R < p$). In this case, it also results that d is greater than d_c (Table 3) and the point representative of this event is located above the critical curve (Figure 10). As a result, a landslide is triggered at the depth considered in accord with what actually observed.

Similar results are obtained when a slip surface located at the depth of 1.40 m is considered. The slope is stable for the first two rainfall events (Figures 11 and 12), whereas a failure occurs owing to the third event (Figure 13). Summarizing, although the first two precipitations were characterized by a higher intensity, the landslide was triggered by the third rainfall event when the initial suction was significantly lower than that measured before the other events considered. These results confirm the importance of the initial suction on the slope stability.

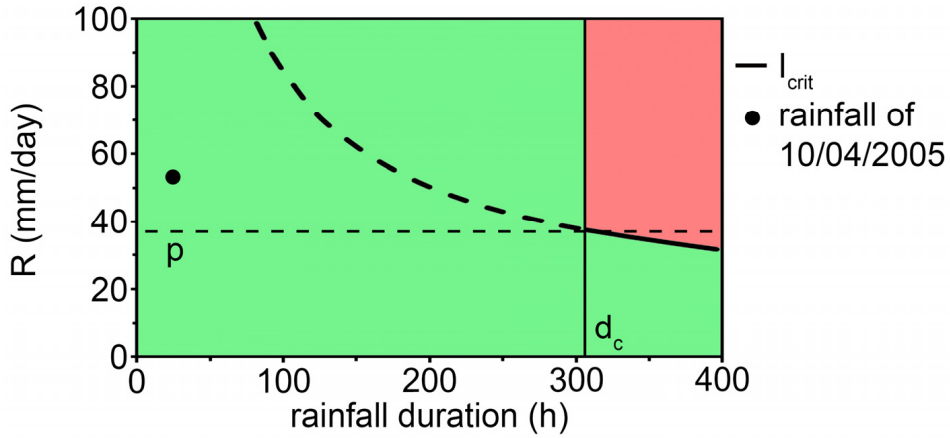

Figure 11. Comparison between the rainfall event recorded on 10 April 2005 and the critical curve calculated at the depth of 1.40 m.

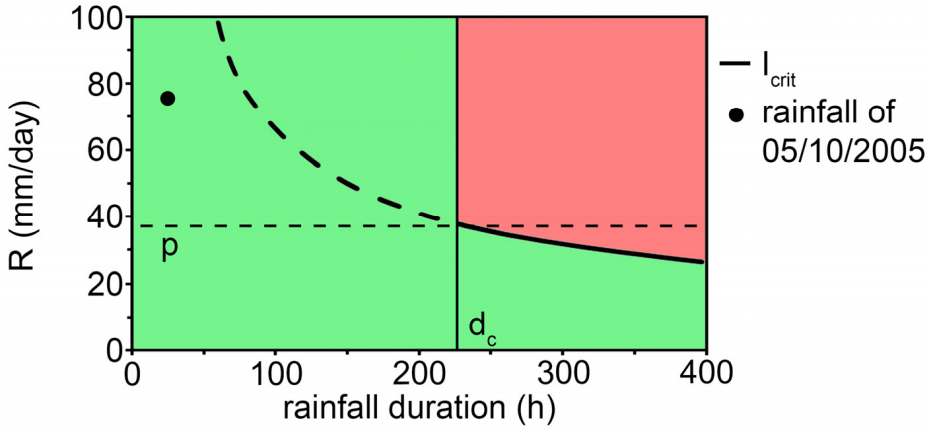

Figure 12. Comparison between the rainfall event recorded on 5 October 2005 and the critical curve calculated at the depth of 1.40 m.

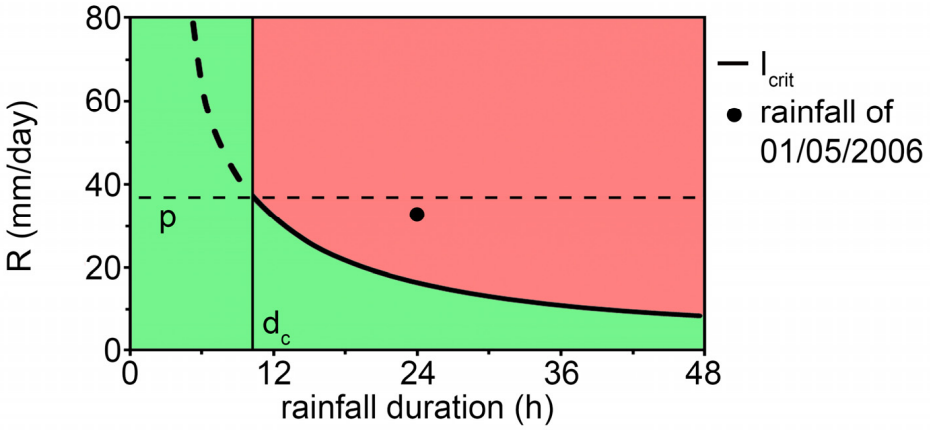

Figure 13. Comparison between the rainfall event recorded on 1 May 2006 and the critical curve calculated at the depth of 1.40 m.

Finally, for the sake of completeness, Figures 14–16 show a comparison between the evolution of u_w calculated at the depth of 0.80 m using Equations (8a) and (8b), and the threshold u_c at the same depth provided by Equation (16). These graphs also allow an evaluation of the time at which failure occurs.

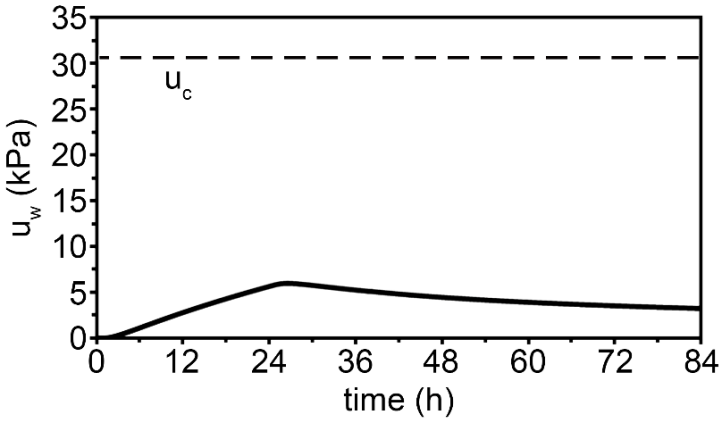

Figure 14. Evolution of the change in pore water pressure, u_w, with time due to the rainfall of 10 April 2005, with indication of the critical threshold, u_c, at the depth of 0.80 m.

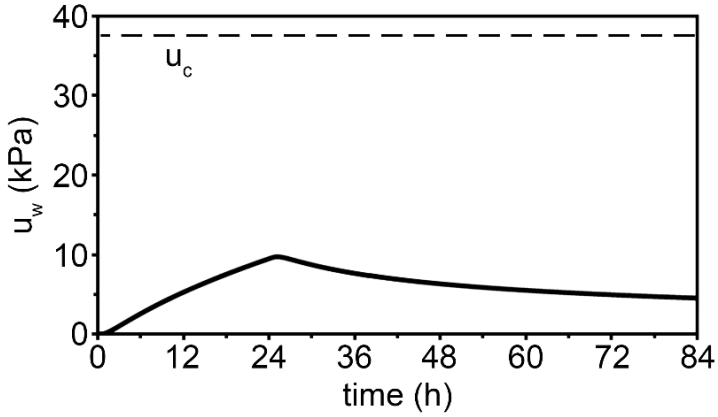

Figure 15. Evolution of the change in pore water pressure, u_w, with time due to the rainfall of 5 October 2005, with indication of the critical threshold, u_c, at the depth of 0.80 m.

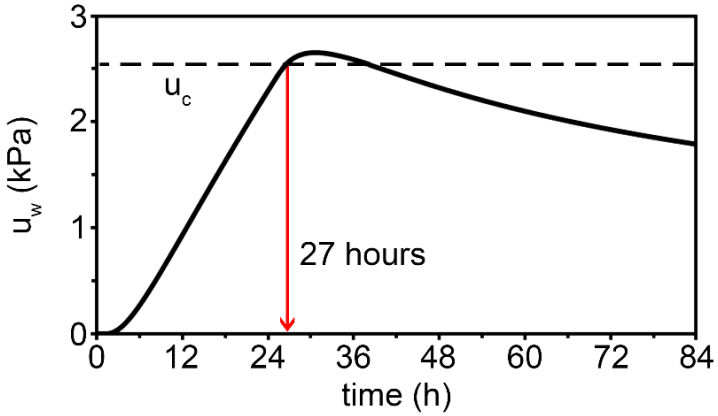

Figure 16. Evolution of the change in pore water pressure, u_w, with time due to the rainfall of 1 May 2006, with indication of the critical threshold, u_c, at the depth of 0.80 m.

In agreement with the results previously shown, the change in pore pressure is always less than its critical value ($u_w < u_c$) for the first two rainfall events (Figures 14 and 15), whereas u_w exceeds u_c owing to the third event (Figure 16). In this last case, a triggering condition ($u_w = u_c$) occurs 27 h after the beginning of the rainfall.

Analogous remarks can be made about the results obtained at the depth of 1.40 m (Figures 17–19). Specifically, the change in pore pressure exceeds the corresponding critical value owing to the third event only. In this case, failure occurs just at the end of the rainfall (i.e., at t = 24 h), preceding that occurred at 0.80 m.

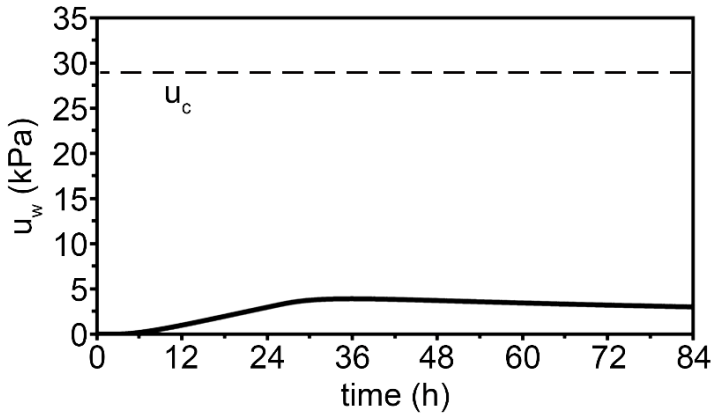

Figure 17. Evolution of the change in pore water pressure, u_w, with time due to the rainfall of 10 April 2005, with indication of the critical threshold, u_c, at the depth of 1.40 m.

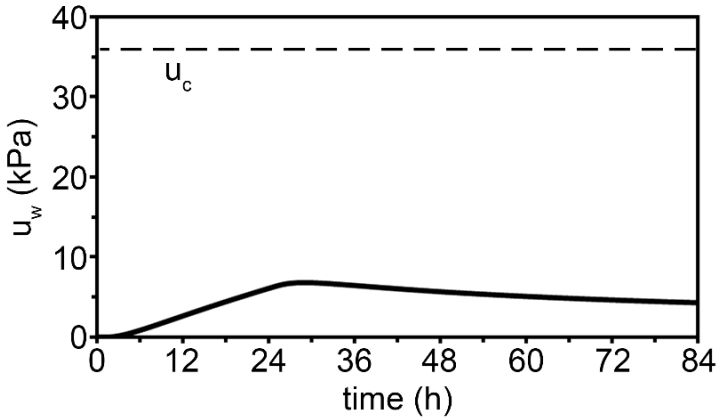

Figure 18. Evolution of the change in pore water pressure, u_w, with time due to the rainfall of 5 October 2005, with indication of the critical threshold, u_c, at the depth of 1.40 m.

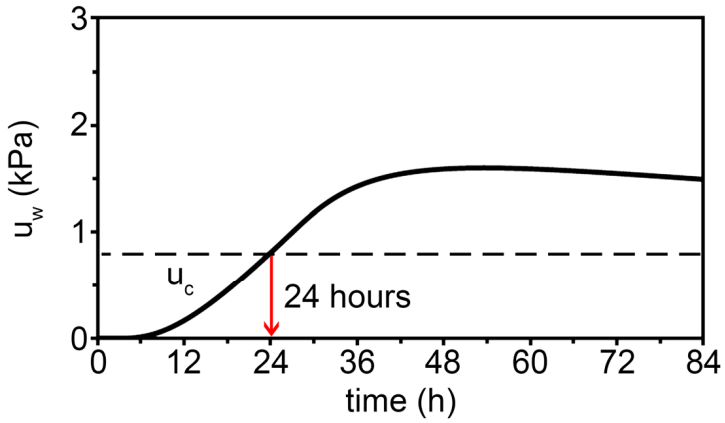

Figure 19. Evolution of the change in pore water pressure, u_w, with time due to the rainfall of 1 May 2006, with indication of the critical threshold, u_c, at the depth of 1.40 m.

The second example is taken from a paper by [54]. This example was inspired by a real case [55] which concerns a shallow landslide occurred in October 1994, in the Province of Girona (North-Eastern Spain) after a period of intense rain. The landslide involved a road embankment and caused soil displacements in the order of some meters. The failure process was simulated by [54] using the Material Point Method (MPM), an advanced and effective numerical technique. The embankment was made up of sandy clay with low to medium plasticity. The available soil properties are summarized in Table 4.

Table 4. Soil properties of the embankment (data from [54,55]).

γ (kN/m^3)	c' (kPa)	ϕ' (°)	k (m/s)
20	0	20	10^{-7}

The soil was unsaturated, and the failure mechanism involved the upper portion of the slope to a depth of about 1.5 m (z = 1.27 m). An infinite slope model with α = 32.5° can be reasonably used to schematize the embankment portion affected by failure (Figure 20).

Measurements of suction are not available. Thus, u_{wo} is estimated in the present study using Equation (17), in which c_t is the initial apparent cohesion assumed by [54] for the involved soil (c_t = 6.7 kPa). The resulting value is $u_{wo} = -18.4$ kPa. The authors of [54] also used the Van Genuchten retention curve [52] to relate the degree of saturation to suction (the parameters of this curve are listed in their Table 4), from which a value of $m_w = 0.00025$ kPa^{-1} is calculated at u_{wo}, under the assumption that the soil void ratio re-

mains unchanged during wetting. In addition, lacking specific experimental data, p is evaluated using Equation (7) from which p = 7.30 mm/day is obtained. Daily rainfall recorded in the period from 1 September to 31 October 1994 are shown in Figure 21. Referring to the rain event with the highest intensity (R = 123 mm/day) and duration d = 24 h, only a portion of this rain can infiltrate into the slope in accordance with Equations (6a) and (6b). In addition, the critical duration is 5.5 h.

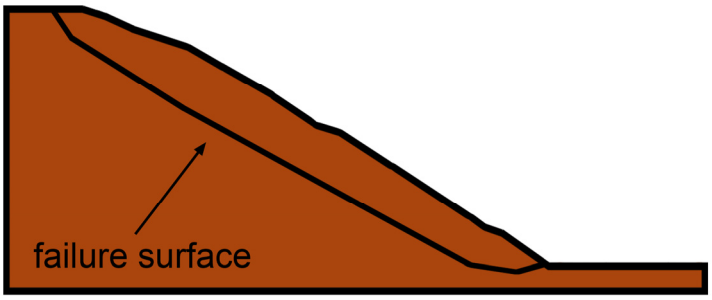

Figure 20. Schematic section of the embankment affected by failure (modified from [55]).

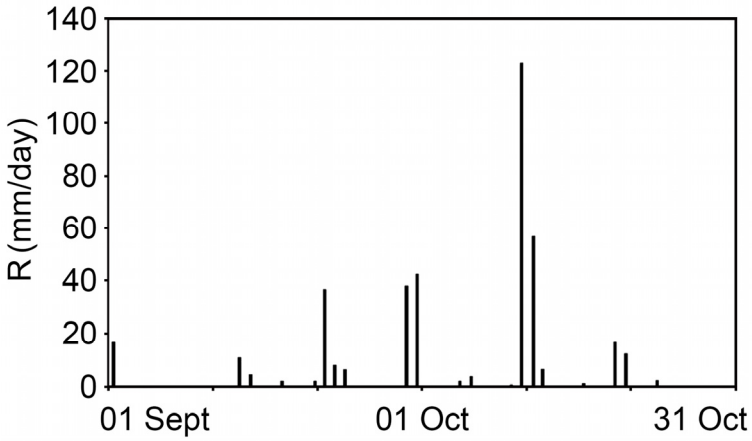

Figure 21. Available rainfall recordings (modified from [55]).

Figure 22 shows the critical curve calculated at a depth of 1.5 m using the proposed method. As can be seen, rainfall duration is greater than the critical one ($d > d_c$) and the point representative of the considered rain event (R = 123 mm/day and d = 24 h) falls into the instability region. This result is consistent with the conclusions of the analysis performed by [54] using MPM.

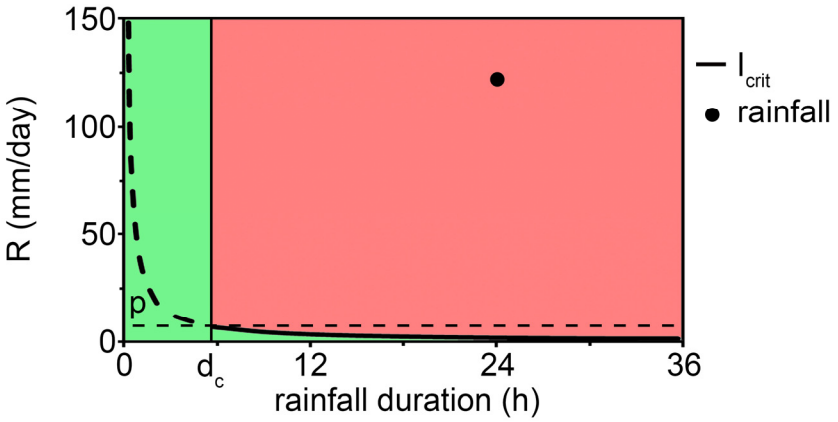

Figure 22. Comparison between the considered rainfall event and the critical curve calculated at the depth of 1.50 m.

4. Discussion

The approach presented in this study allows a preliminary prediction of the occurrence of rainfall-induced shallow landslides in unsaturated soils due to expected rainfall scenarios, under the hypothesis that the rainfall intensity is constant over time. Basically, it is developed referring to the scale of slope. Indeed, the specific characteristics of the considered slope are taken into account, such as geometry, geotechnical properties and suction existing at the depth of the failure surface before rainfall. These characteristics make the method suitable to be employed in the context of an early warning system.

The method is inspired from other studies published in the literature [19,39]. However, novel aspects are introduced in the present work. Compared to [39], the present paper is aimed to the prediction of rainfall-induced shallow landslides in unsaturated soils by the employment of some critical curves of analytical derivation, which are not considered in [39]. Compared to the paper [19], the relationship between the time at which the change in pore water pressure takes the peak value (t_p) and rainfall duration (d) is presented. It is shown that this relationship is a function of depth and hydraulic conductivity. In particular, t_p could be significantly greater than d when depth increases and hydraulic conductivity reduces (Figure 2). As a result, the evolution of u_w with time takes a different shape (Figure 3). In addition, this paper introduces the concept of critical duration which represents a threshold value of rainfall duration below which a landslide cannot occur. This threshold is very useful for practical purposes.

The solution procedure is very simple-to-use and is hence suitable for routine applications. However, the proposed approach is characterized by some approximate assumptions that have to be kept in mind when it is applied to real cases. Specifically, the method is based on a simplified hydrological model and an infinite slope scheme with constant slope angle, thickness, and homogeneous soil properties. Although these assumptions are generally accepted in engineering practice for the analysis of shallow landslides, the proposed method must be used with caution when the slope consists of markedly anisotropic and heterogeneous soils or is characterized by a complex geometry requiring two or three-dimensional hydromechanical models. The proposed method is suitable to analyze the triggering condition of rainfall-induced shallow landslides when the failure surface develops in the unsaturated portion of the slope. On the contrary, when the failure surface concerns the saturated zone, a different approach has to be employed [19,20]. In addition, the proposed model should be applicable for slopes under wet conditions as usually occurs during the rainy periods when the soil is close to saturation and the changes in the involved soil parameters are generally not significant. On the contrary, this model could not be effective for drier slopes when the soil properties strongly depend on suction. In this regard, a study is currently underway to extend the present method to these conditions. In addition, it is worth noting that the value of the suction measured at the depth of the failure surface before rainfall, u_{wo}, plays a crucial role on the slope stability. Therefore, it appears clear that u_{wo} has to be carefully evaluated at the depths of interest using suitable in situ or laboratory measurements. Finally, since the initial suction often varies with depth, the method could be employed to assess the slope stability at the different depths where the initial suction is known, using for any depth the corresponding value of suction.

5. Conclusions

A method of practical interest is presented for predicting rainfall-induced shallow landslide triggering in unsaturated soils. The proposed method is based on some analytical solutions for evaluating the change in suction due to rain infiltration, and the simple scheme of infinite slope to calculate a threshold of the suction change that determines a condition of incipient failure of the slope. Specifically, the approach provides a critical curve defining the rainfall events that are able to trigger a failure mechanism at a given depth where suction existing before rainfall is known. Substantially, the method directly relates landslide occurrence to the intensity and duration of an expected rainfall. In addition, a critical value of the rainfall duration can be readily evaluated, below which no slope

failure occurs at the considered depth. The method is very simple to use and can be easily implemented in a common electronic sheet. Moreover, few parameters are required as input data, which in addition can be obtained from conventional tests. All these features make the proposed method fairly attractive for predictive purposes, as also confirmed by the applications shown in the paper to some case studies documented in the literature.

Author Contributions: Conceptualization, A.T., L.P. and E.C.; Writing—original draft, A.T., L.P. and E.C.; Writing—review & editing, A.T., L.P. and E.C. All authors have read and agreed to the published version of the manuscript.

Funding: This research was funded by "Fondo Sociale Europeo REACT-EU Programma Operativo Nazionale (PON) Ricerca e Innovazione 2014–2020".

Institutional Review Board Statement: Not applicable.

Informed Consent Statement: Not applicable.

Data Availability Statement: The data presented in this study are available on request from the corresponding author.

Conflicts of Interest: The authors declare no conflict of interest.

References

1. Cruden, D.M.; Varnes, D.J. *Landslides—Investigation and Mitigation*; Special Report No. 247, Transportation Research Board; National Academy Press: Washington, DC, USA, 1996.
2. Campbell, R.H. *Soil Slips, Debris Flows, and Rainstorms in the Santa Monica Mountains and Vicinity, Southern California*; US Geological Survey Professional Paper; United States Government Printing Office: Washington, DC, USA, 1975; Volume 851.
3. Eckersley, D. Instrumented laboratory flow slides. *Géotechnique* **1990**, *40*, 489–502. [CrossRef]
4. Olivares, L.; Picarelli, L. Shallow flowslides triggered by intense rainfalls on natural slopes covered by loose unsaturated pyroclastic soils. *Géotechnique* **2003**, *53*, 283–287. [CrossRef]
5. Cascini, L.; Cuomo, S.; Sorbino, G. Flow-like mass movements in pyroclastic soils: Remarks on the modelling of triggering mechanisms. *Ital. Geotech. J.* **2005**, *39*, 11–31.
6. Picarelli, L.; Olivares, L.; Comegna, L.; Damiano, E. Mechanical aspects of flow-like movements in granular and fine grained soils. *Rock Mech. Rock Eng.* **2008**, *41*, 179–197. [CrossRef]
7. Hungr, O.; Leroueil, S.; Picarelli, L. The Varnes classification of landslide types, an update. *Landslides* **2014**, *11*, 167–194. [CrossRef]
8. Troncone, A.; Pugliese, L.; Lamanna, G.; Conte, E. Prediction of rainfall-induced landslide movements in the presence of stabilizing piles. *Eng. Geol.* **2021**, *288*, 106143. [CrossRef]
9. Troncone, A.; Pugliese, L.; Parise, A.; Conte, E. Prediction of Slow-Moving Landslide Mobility Due to Rainfall Using a Two-Wedges Model. *Water* **2021**, *13*, 2030. [CrossRef]
10. Montrasio, L.; Valentino, R. Experimental analysis and modelling of shallow landslides. *Landslides* **2007**, *4*, 291–296. [CrossRef]
11. Van Asch, T.W.J.; Van Beek, L.P.H.; Bogaard, T.A. Problems in predicting the mobility of slow-moving landslides. *Eng. Geol.* **2007**, *91*, 46–55. [CrossRef]
12. Guzzetti, F.; Peruccacci, S.; Rossi, M.; Stark, C. The rainfall intensity-duration control of shallow landslides and debris flow: On update. *Landslides* **2008**, *5*, 3–17. [CrossRef]
13. Cascini, L.; Cuomo, S.; Pastor, M.; Sorbino, G. Modeling of Rainfall-Induced Shallow Landslides of the Flow Types. *J. Geotech. Geoenviron. Eng. ASCE* **2010**, *136*, 85–98. [CrossRef]
14. Pagano, L.; Picarelli, L.; Rianna, G.; Urciuoli, G. A simple numerical procedure for timely prediction of precipitation-induced landslides in unsaturated pyroclastic soils. *Landslides* **2010**, *7*, 273–289. [CrossRef]
15. Conte, E.; Troncone, A. Analytical Method for Predicting the Mobility of Slow-Moving Landslides owing to Groundwater Fluctuations. *J. Geotech. Geoenviron. Eng. ASCE* **2011**, *137*, 777–784. [CrossRef]
16. Askarinejad, A.; Casini, F.; Bischof, P.; Springman, S.F. Rainfall induced instabilities: A field experiment on a silty sand slope in northern Switzerland. *Ital. Geotech. J.* **2012**, *3*, 50–71.
17. Conte, E.; Troncone, A. Stability analysis of infinite clayey slopes subjected to pore pressure changes. *Géotechnique* **2012**, *62*, 87–91. [CrossRef]
18. Conte, E.; Donato, A.; Troncone, A. A simplified method for predicting rainfall-induced mobility of active landslides. *Landslides* **2017**, *14*, 35–45. [CrossRef]
19. Conte, E.; Pugliese, L.; Troncone, A. A Simple Method for Predicting Rainfall-Induced Shallow Landslides. *J. Geotech. Geoenviron. Eng. ASCE* **2022**, *148*, 4022079. [CrossRef]
20. Troncone, A.; Pugliese, L.; Conte, E. Rainfall Threshold for Shallow Landslide Triggering Due to Rising Water Table. *Water* **2022**, *14*, 2966. [CrossRef]
21. Fredlund, D.G.; Rahardjo, H. *Soil Mechanics for Unsaturated Soils*; Wiley: New York, NY, USA, 1993; p. 500, ISBN 978-0-471-85008-3.

22. Khire, M.V.; Benson, C.H.; Bosscher, P.J. Capillary barriers: Design variables and water balance. *J. Geotech. Geoenviron. Eng.* **2000**, *126*, 695–708. [CrossRef]
23. Paronuzzi, P.; Del Fabbro, M.; Bolla, A. Soil moisture profiles of unsaturated colluvial slopes susceptible to rainfall-induced landslides. *Geosciences* **2022**, *12*, 6. [CrossRef]
24. Peranič, J.; Mihalič Arbanas, S.; Arbanas, Z. Importance of the unsaturated zone in landslide reactivation on flysch slopes: Observations from Valiči Landslide, Croatia. *Landslides* **2021**, *18*, 3737–3751. [CrossRef]
25. Yang, K.-H.; Uzuoka, R.; Thuo, J.N.; Lin, G.-L.; Nakai, Y. Coupled hydro-mechanical analysis of two unstable unsaturated slopes subject to rainfall infiltration. *Eng. Geol.* **2017**, *216*, 13–30. [CrossRef]
26. Zhang, J.; Zhu, D.; Zhang, S. Shallow slope stability evolution during rainwater infiltration considering soil cracking state. *Comput. Geotech.* **2020**, *117*, 103285. [CrossRef]
27. Troncone, A.; Pugliese, L.; Parise, A.; Conte, E. A simple method to reduce mesh dependency in modelling landslides involving brittle soils. *Géotech. Lett.* **2022**, *12*, 167–173. [CrossRef]
28. Di Maio, C.; Vassallo, R.; Vallario, M.; Pascale, S.; Sdao, F. Structure and kinematics of a landslide in a complex clayey formation of the Italian Southern Apennines. *Eng. Geol.* **2010**, *116*, 311–322. [CrossRef]
29. Lollino, P.; Santaloia, F.; Amorosi, A.; Cotecchia, F. Delayed failure of quarry slopes in stiff clays: The case of the Lucera landslide. *Géotechnique* **2011**, *61*, 861–874. [CrossRef]
30. Conte, E.; Donato, A.; Pugliese, L.; Troncone, A. Analysis of the Maierato landslide (Calabria, Southern Italy). *Landslides* **2018**, *15*, 1935–1950. [CrossRef]
31. Conte, E.; Pugliese, L.; Troncone, A. Post-failure stage simulation of a landslide using the material point method. *Eng. Geol.* **2019**, *253*, 149–159. [CrossRef]
32. Troncone, A.; Conte, E.; Pugliese, L. Analysis of the Slope Response to an Increase in Pore Water Pressure Using the Material Point Method. *Water* **2019**, *11*, 1446. [CrossRef]
33. Su, X.; Xia, X.; Liang, Q.; Hou, J. A coupled discrete element and depth-averaged model for dynamic simulation of flow-like landslides. *Comput. Geotech.* **2022**, *141*, 104537. [CrossRef]
34. Conte, E.; Pugliese, L.; Troncone, A. Post-failure analysis of the Maierato landslide using the material point method. *Eng. Geol.* **2020**, *277*, 105788. [CrossRef]
35. Troncone, A.; Pugliese, L.; Conte, E. Analysis of an excavation-induced landslide in stiff clay using the material point method. *Eng. Geol.* **2022**, *296*, 106479. [CrossRef]
36. Troncone, A.; Pugliese, L.; Conte, E. Run-out simulation of a landslide triggered by an increase in the groundwater level using the material point method. *Water* **2020**, *12*, 2817. [CrossRef]
37. Pu, J.H.; Tait, S.; Guo, Y.; Huang, Y.; Hanmaiahgari, P.R. Dominant features in three-dimensional turbulence structure: Comparison of non-uniform accelerating and decelerating flows. *Environ. Fluid Mech.* **2018**, *18*, 395–416. [CrossRef]
38. Pu, J.H. Velocity Profile and Turbulence Structure Measurement Corrections for Sediment Transport-Induced Water-Worked. *Bed. Fluids* **2021**, *6*, 86. [CrossRef]
39. Conte, E.; Troncone, A. A method for the analysis of soil slips triggered by rainfall. *Géotechnique* **2012**, *62*, 187–192. [CrossRef]
40. Conte, E.; Cosentini, R.M.; Troncone, A. Shear and dilatational wave velocities for unsaturated soils. *Soil Dyn. Earthq. Eng.* **2009**, *29*, 946–952. [CrossRef]
41. Conte, E.; Cosentini, R.M.; Troncone, A. Geotechnical parameters from Vp and Vs measurements in unsaturated soils. *Soils Found.* **2009**, *49*, 689–698. [CrossRef]
42. Tarantino, A.; Di Donna, A. Mechanics of unsaturated soils: Simple approaches for routine engineering practice. *Ital. Geotech. J.* **2019**, *4*.
43. Wilson, G.W.; Fredlund, D.G.; Barbour, S.L. Coupled soil-atmosphere modeling for soil evaporation. *Can. Geotech. J.* **1994**, *31*, 151–161. [CrossRef]
44. Blight, G.E. Interaction between the atmosphere and the Earth. *Géotechnique* **1997**, *47*, 715–766.
45. Leroueil, S. Natural slopes and cuts: Movement and failure mechanisms. *Géotechnique* **2001**, *51*, 197–243. [CrossRef]
46. Conte, E.; Troncone, A. Simplified Approach for the Analysis of Rainfall-Induced Shallow Landslides. *J. Geotech. Geoenviron. Eng.* **2012**, *138*, 398–406. [CrossRef]
47. Carlslaw, H.L.; Jaeger, J.C. *Conduction of Heat in Solids*; Oxford University Press: Oxford, UK, 1959; p. 522, ISBN 9780198533689.
48. Iverson, R.M. Landslide triggering by rain infiltration. *Water Resour. Res.* **2000**, *36*, 1897–1910. [CrossRef]
49. Fredlund, D.G.; Xing, A.; Fredlund, M.D.; Barbour, S.L. The relationship of the unsaturated soil shear strength to the soil-water characteristic curve. *Can. Geotech. J.* **1996**, *33*, 440–448. [CrossRef]
50. Bittelli, M.; Valentino, R.; Salvatorelli, F.; Rossi Pisa, P. Monitoring soil-water and displacement conditions leading to landslide occurrence in partially saturated clays. *Geomorphology* **2012**, *173–174*, 161–173. [CrossRef]
51. Tosi, M. Root tensile strength relationships and their slope stability implications of three shrub species in the Northern Apennines (Italy). *Geomorphology* **2007**, *87*, 268–283. [CrossRef]
52. Van Genuchten, M.T. A closed-form equation for predicting the hydraulic conductivity of unsaturated soils. *Soil Sci. Soc. Am.* **1980**, *44*, 892–898. [CrossRef]
53. Lu, N.; Godt, J.W.; Wu, D.T. A closed-form equation for effective stress in unsaturated soil. *Water Resour. Res.* **2010**, *46*, W05515. [CrossRef]
54. Yerro, A.; Alonso, E.E.; Pinyol, N.M. The material point method for unsaturated soils. *Géotechnique* **2015**, *65*, 201–217. [CrossRef]
55. Alonso, E.E.; Pinyol, N.M.; Purzin, A.M. *Geomechanics of Failures. Advanced Topics*; Springer: Dordrecht, The Netherlands, 2010.